

Global Cerebral Ischemia-induced Depression Accompanies Alteration of Neuronal Excitability in the Infralimbic Cortex Layer 2/3 Pyramidal Neurons

Dong Cheol Jang¹, Seunghwan Choi², Geehoon Chung¹ and Sun Kwang Kim^{1,2*}

¹Department of Physiology, College of Korean Medicine, Kyung Hee University, Seoul 02447,

²Department of East-West Medicine, Graduate School, Kyung Hee University, Seoul 02447, Korea

Cerebral ischemia can lead to a range of sequelae, including depression. The pathogenesis of depression involves neuronal change of the medial prefrontal cortex (mPFC). However, how cerebral ischemia-induced changes manifest across subregions and layers of the mPFC is not well understood. In this study, we induced cerebral ischemia in mice via transient bilateral common carotid artery occlusion (tBCCAO) and observed depressive-like behavior. Using whole-cell patch clamp recording, we identified changes in the excitability of pyramidal neurons in the prelimbic cortex (PL) and infralimbic cortex (IL), the subregions of mPFC. Compared to sham control mice, tBCCAO mice showed significantly reduced neuronal excitability in IL layer 2/3 but not layer 5 pyramidal neurons, accompanied by increased rheobase current and decreased input resistance. In contrast, no changes were observed in the excitability of PL layer 2/3 and layer 5 pyramidal neurons. Our results provide a new direction for studying the pathogenesis of depression following ischemic damage by showing that cerebral ischemia induces subregion- and layer-specific changes in the mPFC pyramidal neurons.

Key words: Cerebral ischemia, Depression, Medial prefrontal cortex, Prelimbic cortex, Infralimbic cortex, Excitability

INTRODUCTION

Cerebral ischemia is a condition in which insufficient blood flow to the brain results in a lack of oxygen and nutrients needed for normal brain function [1]. Being a major cause of stroke and other cerebrovascular diseases [2], cerebral ischemia results in brain damage that can induce various neurological symptoms including mood disorders. Patients often report depression following the experience of cerebral ischemia. For example, post-stroke depression (PSD) is one of the most prevalent sequelae in stroke patients [3-7]. Growing evidence also indicates that vascular depression (VD) [8,

9] is critically involved in the condition of cerebrovascular disease [10, 11]. Although the brain changes that directly cause PSD and VD are not fully elucidated, the affected brain circuitry appears to be similar to that of major depressive disorder (MDD) [12].

A representative brain region is the medial prefrontal cortex (mPFC) [13]. Structural changes in the mPFC region have been reported in depressed patients [14, 15], as well as animal models of depression [15-17]. Studies found that the dendritic development in the mPFC neuron is affected in mouse models of depression induced by chronic stress exposure, and altering the excitability of mPFC pyramidal neurons affects depressive-like behavior [18, 19].

In rodents, the mPFC comprises subregions: the prelimbic cortex (PL), and the infralimbic cortex (IL). Each mPFC subregion innervates different brain regions and plays distinct roles in aversion [20-24], and PL and IL are mainly involved in depression. Studies have reported the subregion-specific effect on depression, as the activation of PL pyramidal neurons has anti-depressive effects [25],

Submitted June 21, 2023, Revised July 19, 2023,
Accepted August 30, 2023

*To whom correspondence should be addressed.
TEL: 82-2-961-0323, FAX: 82-2-961-0333
e-mail: skkim77@khu.ac.kr

whereas the activation of IL pyramidal neurons has pro-depressive effects [19, 26]. Other studies have focused on the layer-specific effects against depression. The pyramidal neurons in layers 2/3 and 5 of the mPFC innervate distinct brain regions and exhibit differential changes in response to chronic social stress [27]. Manipulation of layer 2/3 pyramidal neurons in the mPFC results in a pro-depressive effect [28], while activation of layer 5 pyramidal neurons produces antidepressive effects [25]. These subregion-specific and layer-specific differences against depression suggest that the neuronal changes in depressive condition might differ among the subregion and layer.

In the context of depression after cerebral ischemia, there also might be subregional- and layer-specific differences. We hypothesized that the changes in the excitability of mPFC neurons accompanying the ischemia-induced depression would manifest differently in the subregion- and layer-specific manner. To investigate the changes in the mPFC, we used the transient bilateral common carotid artery occlusion (tBCCAO) model to induce global cerebral ischemia (GCI) in mice. We then investigated changes in neuronal excitability in layer 2/3 and layer 5 pyramidal neurons in the mPFC subregions PL and IL. We found that only layer 2/3 pyramidal neurons in the IL showed significant alterations in firing frequency, rheobase current, and input resistance. The IL layer 5 pyramidal neurons did not show significant changes. In the PL, neither layer 2/3 nor 5 pyramidal neurons showed significant changes in firing frequency and intrinsic properties. Our findings suggest that neural circuits containing layer 2/3 pyramidal neurons in the IL are specifically affected after cerebral ischemia, implying the distinct role of this region in the pathogenesis of sequelae.

MATERIALS AND METHODS

Animals and surgery

All animal experiments were performed in accordance with the protocols approved by the Animal Care and Use Committee of Kyung Hee University (KHSASP-22-302). Eight-week-old male C57BL/6 mice were purchased from Daehan Bio Link (DBL, Korea). The mice were housed in cages with food and water ad libitum. The room was maintained under a 12-h light/dark cycle and kept at $21 \pm 1^\circ\text{C}$.

The tBCCAO surgery was performed using previously described techniques [29]. Mice were anesthetized under isoflurane inhalation. An incision was made on the ventral neck to expose the major arteries in the anterior cervical area. The common carotid arteries (CCA) were dissected from the surrounding tissues. Aneurysmal clips were placed to occlude the bilateral CCA and were maintained for 25 min. After the clips were removed, we checked

the reperfusion and absence of hemorrhage. Sham procedures were performed with the same anesthesia and surgical protocols but kept the CCAs intact. After the procedure, the animals were returned to a warming box for recovery.

Behavior tests

Forced swimming test (FST)

The testing procedure was based on a previous study [30]. Behavioral tests were conducted in a separate dimly lit room with white noise. The home cage was transferred to the testing room 1 hour prior to the test. Mice were placed in a transparent plastic cylinder (height: 30 cm, diameter: 20 cm) filled with water for 6 minutes. Plastic walls were placed around the cylinder to prevent visual cues. Water temperature was maintained at $24 \pm 1^\circ\text{C}$ and replaced before each session. Mice could swim or float without touching the bottom. Behavior was recorded using a video camera (HDR-CX405, Sony, Tokyo, Japan) and analyzed later. Immobility time was defined as the duration without movements other than those necessary to maintain balance and keep the head above water.

Sucrose preference test (SPT)

The assessments were based on previous studies [31, 32]. Mice were housed alone with two water bottles: one with normal water and another with 1% sucrose solution. Both solutions were warmed to room temperature for 1 hour before placing. To eliminate any preference for the location of the water bottle, the bottles were randomly positioned. Bottle weights were measured before and after the 24-hour experiment to determine liquid consumption. Sucrose preference (%) was calculated as a ratio of sucrose intake to total intake.

Slice preparation and whole-cell recording

Coronal slices of the medial prefrontal cortex (300 μm) were obtained by cutting with a vibratome slicer (Leica, VT1200). The brain was cut in ice-cold NMDG cutting solution containing the following (in mM): 92 NMDG, 92 HCl, 2.5 KCl, 1.2 $\text{NaH}_2\text{PO}_4 \cdot \text{H}_2\text{O}$, 20 HEPES, 5 sodium ascorbate, 2 Thiourea, 3 Sodium pyruvate, 10 $\text{MgSO}_4 \cdot 7\text{H}_2\text{O}$, 0.5 $\text{CaCl}_2 \cdot 2\text{H}_2\text{O}$, 30 NaHCO_3 , 25 Glucose (pH 7.3). Slices were transferred to a recovery chamber containing NMDG-cutting solution kept at 32°C for 10 minutes and then incubated for a further 1 h at room temperature in low-sodium holding solution containing the following (in mM): 75 NaCl, 2.5 KCl, 1.2 $\text{NaH}_2\text{PO}_4 \cdot \text{H}_2\text{O}$, 20 HEPES, 5 sodium ascorbate, 2 Thiourea, 3 Sodium pyruvate, 2 $\text{MgSO}_4 \cdot 7\text{H}_2\text{O}$, 2 $\text{CaCl}_2 \cdot 2\text{H}_2\text{O}$, 30 NaHCO_3 , 25 Glucose (pH 7.3).

Brain slices were placed in a recording chamber on an Olympus

microscope (BX50WI) stage and perfused with standard artificial cerebrospinal fluid containing the following (in mM): 125 NaCl, 2.5 KCl, 1.25 NaH_2PO_4 , 1 $\text{MgCl}_2 \cdot 6\text{H}_2\text{O}$, 2 $\text{CaCl}_2 \cdot 2\text{H}_2\text{O}$, 26 NaHCO_3 , 10 glucose. EPC10 amplifier with PatchMaster software (HEKA Elektronik) were used to amplify signals. Signals were collected with 20 kHz sampling frequency and filtered at 2 kHz. Patch pipettes (4–6 M Ω) were pulled from borosilicate glass and filled with internal solution containing the following: 120 KMeSO₃, 3 KCl, 4 NaCl, 9 HEPES, 0.18 EGTA, 4 Mg-ATP, 0.3 Na-GTP, 10 Na-Phosphocreatine (pH 7.25 adjusted with KOH, ~290 mOsm). During the recording, we did not apply any synaptic blockers to record their natural state of neuronal excitability. All recordings were performed at 32°C. The whole-cell was made after the bridge balance was compensated and membrane potentials were not corrected for the liquid junction potential (10.6 mV at 32°C). The excitability of the pyramidal neuron was measured by applying depolarizing current injection from 0 pA to +300 pA with increments of +50 pA for 500 ms. The voltage sag and input resistance (R_{in}) were measured by applying hyperpolarizing current injection from 0 pA to -300 pA with increments of -50 pA for 800 ms. The experimenter was blind to the surgery condition during the whole experiment.

Data analysis and statistics

The analysis of action potential (AP) has been done with the +300 pA current injection data. The AP onset time was measured by calculating the time delay from the acquisition of the current

injection to the first spike. The AP threshold was determined by measuring the membrane potential where its velocity entered the range of 30–60 mV/ms [33, 34]. AP amplitude was calculated as a difference between the threshold and positive peak. The full width at half maximum (FWHM) of AP was measured by calculating the time duration at the half maximum voltage of AP. The medium afterhyperpolarization (mAHP) was calculated as the voltage difference between the negative peak after the spike train and -70 mV baseline. The fast afterhyperpolarization (fAHP) was measured by subtracting the negative peak of AP from the AP threshold. The amount of voltage sag was determined as the difference between the lowest peak and steady-state voltage during the hyperpolarizing current injection, and the R_{in} was calculated from the steady-state voltage and injected hyperpolarizing current. All data were imported and analyzed by custom-built Python analysis code.

All statistical analyses were performed using Graphpad Prism 9. Two sample t-test and the two-way ANOVA test were used. All graphs are shown as mean \pm SEM. The asterisks *, **, and *** indicate $p < 0.05$, $p < 0.01$, and $p < 0.001$, respectively. Detailed statistical methods and sample numbers for each experiment are written in the figure legends.

RESULTS

The tBCCAO surgery was performed on experimental animals to induce cerebral ischemia (Fig. 1A). The tBCCAO is a well-established experimental approach for inducing ischemic damage

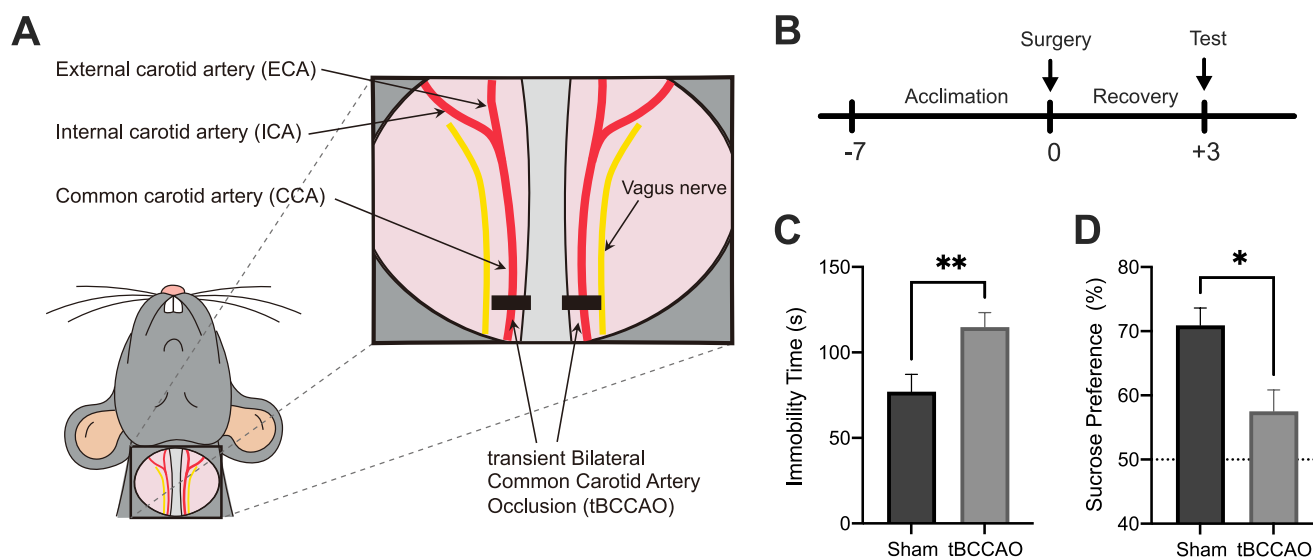


Fig. 1. Depressive-like behavior after tBCCAO. (A) Schematic flow of surgery and behavioral test. (B) Immobility time during forced swimming test (FST). The tBCCAO group showed a significantly longer immobility time than the sham control group (sham=19, tBCCAO=27, $p=0.007$). (C) Sucrose preference between tBCCAO and sham control group. (D) The tBCCAO group showed significantly lower sucrose preference than the sham control (sham=9, tBCCAO=16, $p=0.012$). * $p < 0.05$, ** $p < 0.01$.

to the brain and causes vascular cognitive impairment [29, 35] or depressive-like behavior [36, 37]. We first tested the successful induction of depressive-like behavior in tBCCAO mice. Animals were randomly assigned to tBCCAO group or sham control group, and behavioral tests were performed 3 days after the surgery (Fig. 1B). As in previous reports, depressive-like behavior appeared in tBCCAO animals in the forced swimming test (FST) and the sucrose preference test (SPT), shown by significantly higher immobility time in FST (Fig. 1C, $p=0.007$) and lower sucrose preference in SPT compared to sham controls (Fig. 1D, $p=0.012$).

We then recorded the excitability of PL pyramidal neurons in a layer-specific manner to compare the tBCCAO group and sham control group. For PL pyramidal neurons, both layer 2/3 and layer 5 showed no significant alterations in firing frequency (Fig. 2C, I), rheobase current (Fig. 2D, J), sag voltage (Fig. 2E, K), and input resistance (Fig. 2F, L). Nevertheless, several intrinsic properties showed significant differences (Table 1). PL layer 2/3 pyramidal neurons of the tBCCAO group had a significantly shorter FWHM ($p=0.015$) and faster AP downstroke speed ($p=0.036$) compared to sham control. In PL layer 5 pyramidal neurons of the tBCCAO group, the AP upstroke speed was significantly faster ($p=0.046$) and mAHP was significantly higher ($p=0.044$) than sham control. The FWHM ($p=0.106$) and AP downstroke speed ($p=0.109$) showed slight differences, although they were not statistically significant. Taken together, these data suggest that layer-specific changes of the intrinsic properties occurred in the pyramidal neurons in the PL of mice that had experienced cerebral ischemia.

Next, we recorded the excitability of IL pyramidal neurons. We found that, unlike PL pyramidal neurons, the firing frequency of layer 2/3 pyramidal neurons in the IL was significantly lower in the tBCCAO group than sham control (Fig. 3C, $p<0.001$). This decrease in firing frequency was accompanied by a significant increase in the rheobase current (Fig. 3D, $p=0.017$) and a reduction in input resistance (Fig. 3F, $p=0.006$), whereas the sag voltage remained unchanged (Fig. 3E, $p=0.428$). Changes were also observed in the other intrinsic properties (Table 2). IL layer 2/3 pyramidal neurons of the tBCCAO group had a significantly longer FWHM ($p=0.040$) and slower AP downstroke speed ($p=0.047$) compared to sham control. In contrast, IL layer 5 pyramidal neurons of the tBCCAO group showed no significant difference in the firing frequency compared to sham control (Fig. 3I, $p=0.090$). Similarly, the rheobase current was not statistically significantly different between groups (Fig. 3J, $p=0.209$). No differences were observed in sag voltage and input resistance (Fig. 3K, L) and in the other intrinsic properties (Table 2). These data demonstrate that tBCCAO-induced ischemic damage specifically affects IL layer 2/3 pyramidal neurons, while layer 5 pyramidal neurons remain unaffected.

Consistent with the data from PL, this again suggests that changes in the intrinsic properties in the mPFC pyramidal neurons following cerebral ischemia occurred in a layer-specific manner.

DISCUSSION

Clinical studies have found that more than a third of ischemic stroke patients have experienced depression [6]. Preclinical studies have developed several rodent models of cerebral ischemia using surgical approaches, including middle cerebral artery occlusion (MCAO), bilateral CCA stenosis (BCAS), and BCCAO [38, 39]. With ischemic damage, the affected experimental animals exhibit depressive-like behaviors [40, 41] and the pro-depressive effects are even greater when combined with chronic stress [42]. However, not all the methods are suitable for depression study, as the animals subjected to the surgery show low survival rates and often accompany motor deficits [42, 43]. We adopted the tBCCAO model in this study, as this method has a higher survival rate than other methods such as MCAO and does not induce motor deficits [29]. Using this model, we successfully observed the depressive symptoms in the experimental animals and measured changes in neuronal excitability in the relevant brain region.

The ischemic damage in the brain regions is involved in the development of abnormal moods such as depression. As with major depressive disorder, the manifestation of depression in cerebrovascular diseases is associated with the mPFC. Generally, the mPFC region plays a crucial role in emotional processing and is strongly associated with mood disorders including depression [13]. Functional and structural abnormalities in this region are known to increase vulnerability to depression [24], and modulating mPFC activity can alter depressive behavior. For example, mice subjected to chronic social defeat stress exhibit a reduction in social interaction and immediate early gene expression in the mPFC, and optogenetic activation of the mPFC restores both social behavior and gene expression [44]. Interestingly, other studies have reported that optogenetic activation of mPFC pyramidal neurons leads to pro-depressive behaviors such as decreased social interaction and sucrose preference [15, 18, 19]. This opposite direction of the reports might stem from the different effects of mPFC subregions, layers and cell types on depression.

We investigated the changes in neuronal excitability following global cerebral ischemia in a layer-specific manner within the IL and PL, the subregions of the mPFC. We found that layer 2/3 pyramidal neurons in the IL showed a significant decrease in firing frequency in tBCCAO animals, with changes in rheobase current and input resistance (Fig. 3). However, no changes were observed in IL layer 5 pyramidal neurons (Fig. 3). In the PL, neither layer

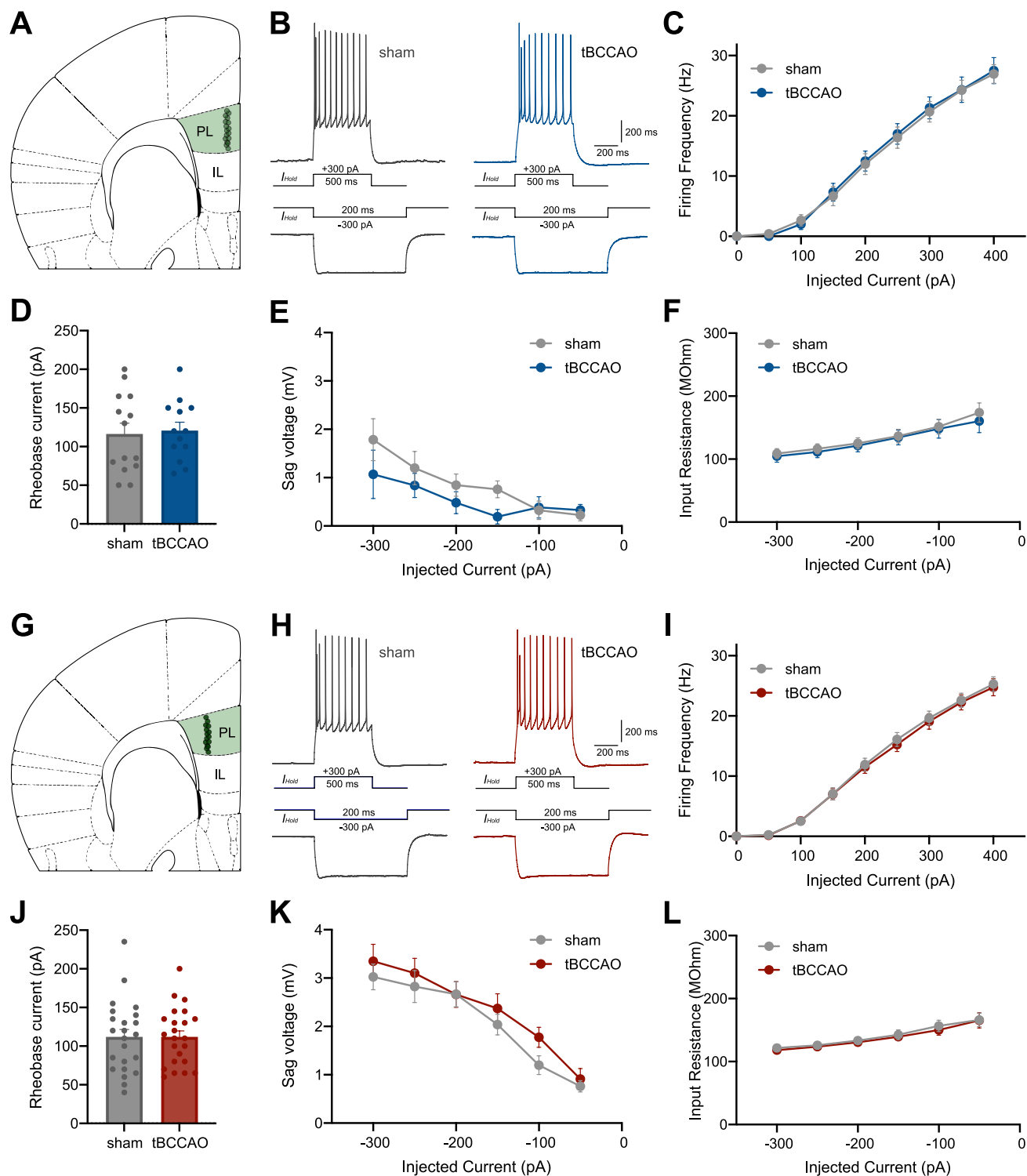


Fig. 2. Prelimbic pyramidal neurons in both layer 2/3 and layer 5 were not altered after tBCCAO. (A) Schematic figure of layer 2/3 neurons in the PL. (B) Representative traces from depolarizing and hyperpolarizing current injection protocol. In PL layer 2/3 neurons, (C) firing frequency and (D) rheobase current of tBCCAO group was comparable to those of sham group (sham=14, tBCCAO=13; firing frequency, $p=0.998$; rheobase current, $p=0.809$). (E) The Sag voltage and (F) input resistance of tBCCAO group were comparable to those of sham group (sham=13, tBCCAO=10; sag voltage, $p=0.388$; input resistance, $p=0.789$). (G) Schematic figure of layer 5 neurons in the PL. (H) Representative traces from depolarizing and hyperpolarizing current injection protocol. In PL layer 5 neurons, (I) firing frequency and (J) rheobase current of tBCCAO group were comparable to those of sham group (sham=23, tBCCAO=23; firing frequency, $p=0.998$; rheobase current, $p=0.999$). (K) Sag voltage and (L) input resistance of tBCCAO group were comparable to those of sham group (sham=23, tBCCAO=23; sag voltage, $p=0.708$; input resistance, $p=0.959$).

Table 1. Intrinsic properties of layer 2/3 and layer 5 pyramidal neurons in the prelimbic cortex

Intrinsic property	Prelimbic cortex					
	Layer 2/3 pyramidal neuron			Layer 5 pyramidal neuron		
	sham	tBCCAO	p value	sham	tBCCAO	p value
AP threshold (mV)	-27.73±1.48	-25.63±1.86	0.368	-30.34±0.95	-29.04±0.96	0.340
AP amplitude (mV)	86.04±0.98	84.20±1.46	0.301	84.77±1.14	86.13±1.25	0.426
FWHM (ms)	0.97±0.04	0.83±0.03	0.015*	0.900±0.04	0.83±0.02	0.106
AP upstroke (V/s)	459.31±25.62	507.43±32.14	0.249	420.16±14.71	465.38±16.39	0.046*
AP downstroke (V/s)	-79.96±3.63	-92.89±4.62	0.036*	-86.12±4.16	-107.75±12.56	0.109
fAHP (mV)	11.06±0.99	11.34±0.67	0.822	9.35±0.65	10.04±0.56	0.426
mAHP (mV)	0.93±0.32	0.87±0.24	0.890	3.18±0.25	4.05±0.34	0.044*
RMP (mV)	-66.52±2.22	-66.64±2.16	0.973	-62.63±1.37	-61.91±1.23	0.725

Layer 2/3 pyramidal neurons (sham=14, tBCCAO=13), layer 5 pyramidal neurons (sham=23, tBCCAO=23). *p<0.05.

2/3 nor layer 5 pyramidal neurons showed significant alterations in firing frequency (Fig. 2), although we observed some minor changes in intrinsic properties such as AP width (Table 1).

Our results primarily suggest that the ischemic condition induced by tBCCAO led to a differential effect on the intrinsic properties of pyramidal neurons in different mPFC subregions, the PL and IL. Previous studies have reported that the PL and IL play distinct roles in behaviors such as pain and active avoidance [22, 45], as well as in mood disorders [46-48]. For instance, activation of the PL induces anxiety-like behavior, while activation of the IL does not change anxiety-like behavior [48]. Additionally, fear conditioning increases the activity of the PL [46] while decreasing the excitability of the IL neurons [47]. In terms of depression, studies have demonstrated that activating the PL pyramidal neurons exerts an anti-depressive effect [25]. The effect of activation of the IL pyramidal neurons is controversial, as both the anti-depressive [49] and the pro-depressive effect have been reported [19, 26]. Thus, more detailed studies beyond subregions would be required for a better understanding of the relationship between IL and PL activity and depression.

The implication of our results is that cerebral ischemia-induced changes in the excitability of pyramidal neurons vary across different layers within the mPFC subregions. Specifically, we observed a reduction in firing frequency only in IL layer 2/3 pyramidal neurons of the tBCCAO group. Previous studies have found that even in the same area, the neuronal responses to the same stimuli can differ depending on the cortical layer. For example, the PL pyramidal neurons show different levels of changes depending on the layer in the condition of chronic stress-induced depression [27] or learned helplessness [50]. Functions and roles of the pyramidal neurons in each layer for depression may also vary. Activation of the mPFC layer 5 neurons produces an anti-depressive effect [25], whereas modulation of layer 2/3 pyramidal neurons increases a vulnerability to stress-induced depression [28]. These might stem

from differences in projection to other brain regions [27] or differences in the expression levels of the receptors that lead to distinct responsiveness to synaptic inputs [51].

We note that we are not claiming that changes in the mPFC subregion selectively affect depression alone. Generally, cerebral ischemia can be accompanied by multiple sequelae beyond depression, such as cognitive impairment or anxiety [29, 52], which are also directly or indirectly related to the mPFC dysfunction. Nevertheless, our observation that only IL layer 2/3 pyramidal neurons show changes in excitability has interesting implications for depression. According to a previous study, selective modulation of layer 2/3 pyramidal neurons in the mPFC caused depressive-like behavior without changes in cognitive function or anxiety [28]. Although the study showed that changes in the activity of mPFC layer 2/3 pyramidal neurons were causally related to depressive-like symptoms, it was not clear which subregion is responsible for depression because the study did not distinguish between subregions of IL and PL. Our observations showed selective changes in IL layer 2/3 pyramidal neurons, suggesting the importance of this region.

In the same vein, we are not claiming that the changes we observed in the mPFC are the only factors responsible for depressive-like symptoms after cerebral ischemia. Previous studies have shown that BCCAO leads to neuronal cell death in the hippocampal CA1 and CA3 regions [53, 54]. It also affected the other regions in the frontal cortex such as the anterior cingulate cortex (ACC) and orbitofrontal cortex, without affecting the mPFC subregions of IL and PL [55]. Changes in these areas other than IL also could contribute to various sequelae of cerebral ischemia, including depression. In this regard, multiple brain regions are involved in depressive-like symptoms, and the mPFC are connected with many relevant regions, including the hippocampus, thalamus, and amygdala [28, 56]. For example, changes in the IL might be attributable to abnormal hippocampal input, given that IL receives more

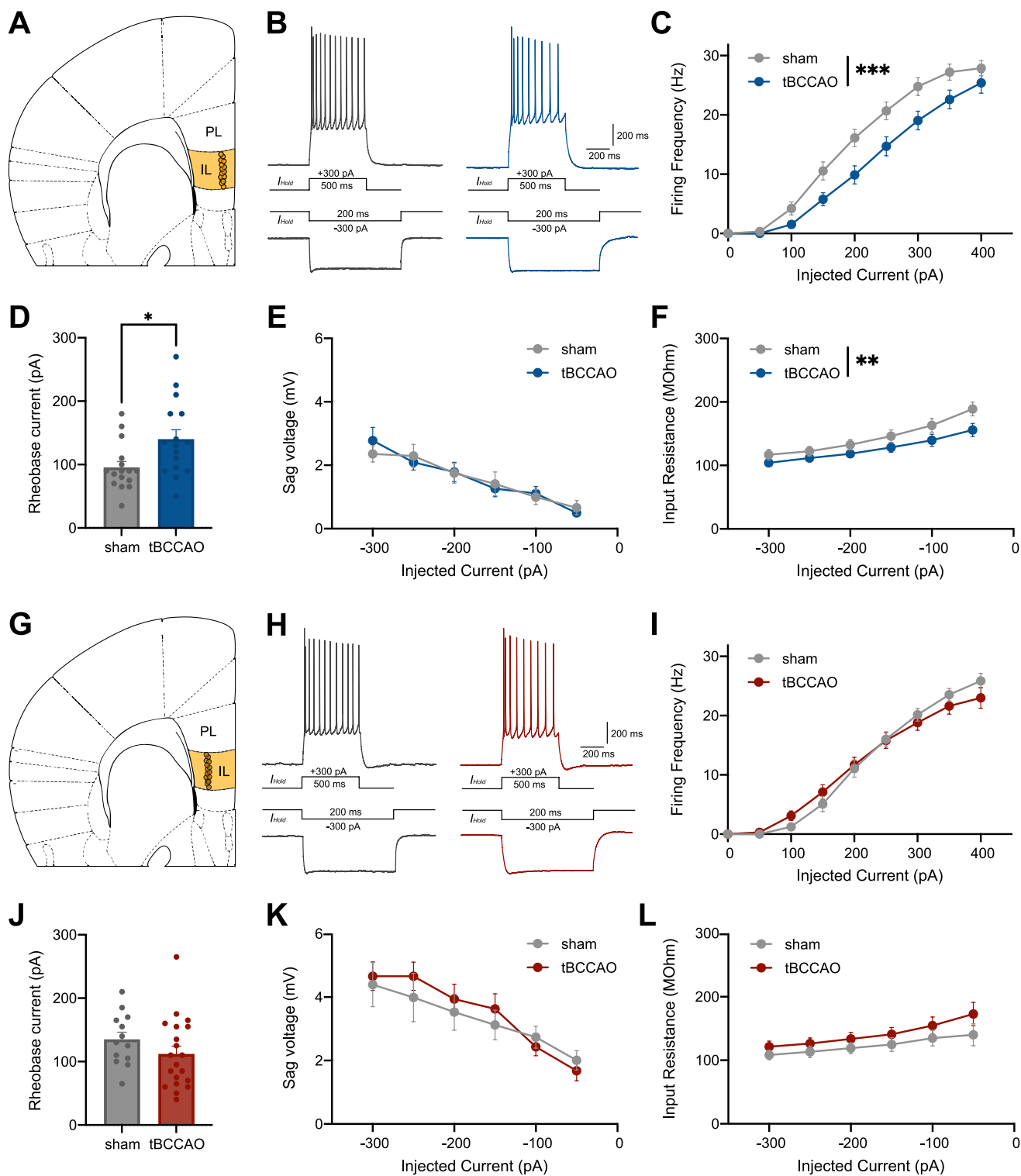


Fig. 3. Only infralimbic pyramidal neurons in layer 2/3 were altered after tBCCAO. (A) Schematic figure of layer 2/3 neurons in the IL. (B) Representative traces from depolarizing and hyperpolarizing current injection protocol. (C) The firing frequency was significantly reduced in the tBCCAO group (sham=18, tBCCAO=17, $p<0.001$). (D) The rheobase current of tBCCAO group was considerably higher than that of sham group ($p=0.017$). (E) Sag voltage of tBCCAO group was comparable to those of sham group (sham=13, tBCCAO=15, $p=0.428$). (F) The input resistance was significantly decreased in the tBCCAO group ($p=0.006$). (G) Schematic figure of layer 5 neurons in the IL. (H) Representative traces from depolarizing and hyperpolarizing current injection protocol. In IL layer 5 neurons, (I) firing frequency and (J) rheobase current of tBCCAO group were comparable to those of sham group (sham=13, tBCCAO=20; firing frequency, $p=0.090$; rheobase current, $p=0.209$). (K) The Sag voltage and (L) input resistance of tBCCAO group were comparable to those of sham group (sham=13, tBCCAO=18; sag voltage, $p=0.187$; input resistance, $p=0.487$). * $p<0.05$, ** $p<0.01$, *** $p<0.001$.

Table 2. Intrinsic properties of layer 2/3 and layer 5 pyramidal neurons in the infralimbic cortex

Intrinsic property	Infralimbic cortex					
	Layer 2/3 pyramidal neuron			Layer 5 pyramidal neuron		
	sham	tBCCAO	p value	sham	tBCCAO	p value
AP threshold (mV)	-22.54±1.64	-21.17±2.36	0.634	-26.60±2.22	-26.74±1.12	0.952
AP amplitude (mV)	85.41±1.54	82.32±1.77	0.195	89.71±2.12	86.04±1.75	0.194
FWHM (ms)	0.84±0.02	0.90±0.02	0.040*	0.79±0.02	0.80±0.02	0.776
AP upstroke (V/s)	496.80±23.45	449.92±27.35	0.208	515.32±25.80	511.16±23.92	0.909
AP downstroke (V/s)	-130.84±17.29	-88.17±10.92	0.047*	-140.59±24.71	-116.85±13.08	0.361
fAHP (mV)	12.57±0.96	13.17±1.06	0.676	10.54±1.18	11.63±0.69	0.403
mAHP (mV)	0.02±0.41	0.55±0.57	0.458	3.30±0.60	3.49±0.51	0.811
RMP (mV)	-65.13±4.62	-63.12±2.67	0.690	-62.93±1.23	-64.12±1.34	0.549

Layer 2/3 pyramidal neurons (sham=18, tBCCAO=17), layer 5 pyramidal neurons (sham=13, tBCCAO=20). *p<0.05.

input from the CA1 compared to the PL [57].

Another factor to note is the influence of excitatory and inhibitory inputs to layer 2/3 neurons. In this study, only changes in excitability were measured in the pyramidal neurons. We did not use any synaptic blockers as we intended to measure the excitability of the pyramidal neurons with intact synaptic inputs. Changes in excitatory and inhibitory influences from surrounding neurons might affect the excitability, but we analyzed only the integrated outputs (i.e., APs) of the neurons being recorded. The mPFC pyramidal neurons are persistently influenced by complex local inhibitory circuitry [58], making it difficult to define a specific mechanism regarding the changes in excitability. Previous reports have shown that inhibitory transmission increases after cerebral ischemia [59], and GABAergic inhibition increases in cortical layer 2/3 pyramidal neurons after stroke [60]. This is consistent with our findings of a selective decrease in the excitability of layer 2/3 pyramidal neurons. Future studies should investigate detailed changes in excitatory and inhibitory synaptic transmission depending on the subregions. Given that changes in inhibitory interneurons have been reported in mouse models of depression [61–63] as well as cerebral ischemia [59, 60, 64], investigating the role of inhibitory interneurons depending on the subregions would be a valuable direction for future research.

ACKNOWLEDGEMENTS

This research was supported by the National Research Foundation of Korea (NRF) grant funded by the Korean government (MSIT) (NRF-2021R1C1C1013840 to D.C.J.; NRF-2020R1C1C1009162 to G.C.; NRF-2019R1A2C2086052 to S.K.K).

REFERENCES

1. Vespa P, Bergsneider M, Hattori N, Wu HM, Huang SC, Martin NA, Glenn TC, McArthur DL, Hovda DA (2005) Metabolic crisis without brain ischemia is common after traumatic brain injury: a combined microdialysis and positron emission tomography study. *J Cereb Blood Flow Metab* 25:763-774.
2. Daniele SG, Trummer G, Hossmann KA, Vrselja Z, Benk C, Gubeske KT, Damjanovic D, Andrijevic D, Pooth JS, Dellal D, Beyersdorf F, Sestan N (2021) Brain vulnerability and viability after ischaemia. *Nat Rev Neurosci* 22:553-572.
3. Loubinoux I, Kronenberg G, Endres M, Schumann-Bard P, Freret T, Filipkowski RK, Kaczmarek L, Popa-Wagner A (2012) Post-stroke depression: mechanisms, translation and therapy. *J Cell Mol Med* 16:1961-1969.
4. Schöttke H, Giabbiconi CM (2015) Post-stroke depression and post-stroke anxiety: prevalence and predictors. *Int Psychogeriatr* 27:1805-1812.
5. Robinson RG, Jorge RE (2016) Post-stroke depression: a review. *Am J Psychiatry* 173:221-231.
6. Towfighi A, Ovbiagele B, El Husseini N, Hackett ML, Jorge RE, Kissela BM, Mitchell PH, Skolarus LE, Whooley MA, Williams LS (2017) Poststroke depression: a scientific statement for healthcare professionals from the American Heart Association/American Stroke Association. *Stroke* 48:e30-e43.
7. Frank D, Gruenbaum BF, Zlotnik A, Semyonov M, Frenkel A, Boyko M (2022) Pathophysiology and current drug treatments for post-stroke depression: a review. *Int J Mol Sci* 23:15114.
8. Alexopoulos GS, Meyers BS, Young RC, Campbell S, Silbersweig D, Charlson M (1997) 'Vascular depression' hypothesis. *Arch Gen Psychiatry* 54:915-922.
9. Thomas AJ, Kalaria RN, O'Brien JT (2004) Depression and vascular disease: what is the relationship? *J Affect Disord*

- 79:81-95.
10. Steffens DC, Helms MJ, Krishnan KR, Burke GL (1999) Cerebrovascular disease and depression symptoms in the cardiovascular health study. *Stroke* 30:2159-2166.
 11. Ramasubbu R (2000) Relationship between depression and cerebrovascular disease: conceptual issues. *J Affect Disord* 57:1-11.
 12. Albert PR (2018) Is poststroke depression the same as major depression? *J Psychiatry Neurosci* 43:76-78.
 13. Bittar TP, Labonté B (2021) Functional contribution of the medial prefrontal circuitry in major depressive disorder and stress-induced depressive-like behaviors. *Front Behav Neurosci* 15:699592.
 14. Kang HJ, Voleti B, Hajszan T, Rajkowska G, Stockmeier CA, Licznarski P, Lepack A, Majik MS, Jeong LS, Banasr M, Son H, Duman RS (2012) Decreased expression of synapse-related genes and loss of synapses in major depressive disorder. *Nat Med* 18:1413-1417.
 15. Hare BD, Duman RS (2020) Prefrontal cortex circuits in depression and anxiety: contribution of discrete neuronal populations and target regions. *Mol Psychiatry* 25:2742-2758.
 16. Li N, Lee B, Liu RJ, Banasr M, Dwyer JM, Iwata M, Li XY, Aghajanian G, Duman RS (2010) mTOR-dependent synapse formation underlies the rapid antidepressant effects of NMDA antagonists. *Science* 329:959-964.
 17. Li N, Liu RJ, Dwyer JM, Banasr M, Lee B, Son H, Li XY, Aghajanian G, Duman RS (2011) Glutamate N-methyl-D-aspartate receptor antagonists rapidly reverse behavioral and synaptic deficits caused by chronic stress exposure. *Biol Psychiatry* 69:754-761.
 18. Yizhar O, Fenno LE, Prigge M, Schneider F, Davidson TJ, O'Shea DJ, Sohal VS, Goshen I, Finkelstein J, Paz JT, Stehfest K, Fudim R, Ramakrishnan C, Huguenard JR, Hegemann P, Deisseroth K (2011) Neocortical excitation/inhibition balance in information processing and social dysfunction. *Nature* 477:171-178.
 19. Ferenczi EA, Zalocusky KA, Liston C, Grosenick L, Warden MR, Amatya D, Katovich K, Mehta H, Patenaude B, Ramakrishnan C, Kalanithi P, Etkin A, Knutson B, Glover GH, Deisseroth K (2016) Prefrontal cortical regulation of brain-wide circuit dynamics and reward-related behavior. *Science* 351:aac9698.
 20. Vertes RP (2004) Differential projections of the infralimbic and prelimbic cortex in the rat. *Synapse* 51:32-58.
 21. Mitrić M, Seewald A, Moschetti G, Sacerdote P, Ferraguti F, Kummer KK, Kress M (2019) Layer- and subregion-specific electrophysiological and morphological changes of the medial prefrontal cortex in a mouse model of neuropathic pain. *Sci Rep* 9:9479.
 22. Kummer KK, Mitrić M, Kalpachidou T, Kress M (2020) The medial prefrontal cortex as a central hub for mental comorbidities associated with chronic pain. *Int J Mol Sci* 21:3440.
 23. Porter JT, Sepulveda-Orengo MT (2020) Learning-induced intrinsic and synaptic plasticity in the rodent medial prefrontal cortex. *Neurobiol Learn Mem* 169:107117.
 24. Pizzagalli DA, Roberts AC (2022) Prefrontal cortex and depression. *Neuropsychopharmacology* 47:225-246.
 25. Kumar S, Black SJ, Hultman R, Szabo ST, DeMaio KD, Du J, Katz BM, Feng G, Covington HE 3rd, Dzirasa K (2013) Cortical control of affective networks. *J Neurosci* 33:1116-1129.
 26. Moreines JL, Owrutsky ZL, Grace AA (2017) Involvement of infralimbic prefrontal cortex but not lateral habenula in dopamine attenuation after chronic mild stress. *Neuropsychopharmacology* 42:904-913.
 27. Bittar TP, Pelaez MC, Hernandez Silva JC, Quessy F, Lavigne AA, Morency D, Blanchette LJ, Arsenault E, Cherasse Y, Seigneur J, Timofeev I, Sephton CF, Proulx CD, Labonté B (2021) Chronic stress induces sex-specific functional and morphological alterations in corticoaccumbal and corticotegmental pathways. *Biol Psychiatry* 90:194-205.
 28. Shrestha P, Mousa A, Heintz N (2015) Layer 2/3 pyramidal cells in the medial prefrontal cortex moderate stress induced depressive behaviors. *Elife* 4:e08752.
 29. Choi S, Jang DC, Chung G, Kim SK (2022) Transcutaneous auricular vagus nerve stimulation enhances cerebrospinal fluid circulation and restores cognitive function in the rodent model of vascular cognitive impairment. *Cells* 11:3019.
 30. Can A, Dao DT, Arad M, Terrillion CE, Piantadosi SC, Gould TD (2012) The mouse forced swim test. *J Vis Exp* 59:e3638.
 31. Eagle AL, Mazei-Robison M, Robison AJ (2016) Sucrose preference test to measure stress-induced anhedonia. *Bio-protocols* 6:e1822.
 32. Liu MY, Yin CY, Zhu LJ, Zhu XH, Xu C, Luo CX, Chen H, Zhu DY, Zhou QG (2018) Sucrose preference test for measurement of stress-induced anhedonia in mice. *Nat Protoc* 13:1686-1698.
 33. Kim CH, Oh SH, Lee JH, Chang SO, Kim J, Kim SJ (2012) Lobule-specific membrane excitability of cerebellar Purkinje cells. *J Physiol* 590:273-288.
 34. Ryu C, Jang DC, Jung D, Kim YG, Shim HG, Ryu HH, Lee YS, Linden DJ, Worley PF, Kim SJ (2017) STIM1 regulates somatic Ca²⁺ signals and intrinsic firing properties of cerebellar Purkinje neurons. *J Neurosci* 37:8876-8894.
 35. Jiwa NS, Garrard P, Hainsworth AH (2010) Experimental

- models of vascular dementia and vascular cognitive impairment: a systematic review. *J Neurochem* 115:814-828.
36. Du B, Li H, Zheng H, Fan C, Liang M, Lian Y, Wei Z, Zhang Y, Bi X (2019) Minocycline ameliorates depressive-like behavior and demyelination induced by transient global cerebral ischemia by inhibiting microglial activation. *Front Pharmacol* 10:1247.
 37. Farajdokht F, Oghbaei F, Sadigh-Eteghad S, Majdi A, Aghsan SR, Farhoudi M, Vahidi-Eyrisofla N, Mahmoudi J (2022) Cerebrolysin® and environmental enrichment, alone or in combination, ameliorate anxiety- and depressive-like behaviors in a post-ischemic depression model in mice. *J Stroke Cerebrovasc Dis* 31:106519.
 38. Bederson JB, Pitts LH, Tsuji M, Nishimura MC, Davis RL, Bartkowski H (1986) Rat middle cerebral artery occlusion: evaluation of the model and development of a neurologic examination. *Stroke* 17:472-476.
 39. Venkat P, Chopp M, Chen J (2015) Models and mechanisms of vascular dementia. *Exp Neurol* 272:97-108.
 40. Kuts R, Melamed I, Shiyntum HN, Frank D, Grinshpun J, Zlotnik A, Brotfain E, Dubilet M, Natanel D, Boyko M (2019) A middle cerebral artery occlusion technique for inducing post-stroke depression in rats. *J Vis Exp* 147:e58875.
 41. Wu C, Zhang J, Chen Y (2015) Study on the behavioral changes of a post-stroke depression rat model. *Exp Ther Med* 10:159-163.
 42. Zhang G, Chen L, Yang L, Hua X, Zhou B, Miao Z, Li J, Hu H, Namaka M, Kong J, Xu X (2015) Combined use of spatial restraint stress and middle cerebral artery occlusion is a novel model of post-stroke depression in mice. *Sci Rep* 5:16751.
 43. Lee NT, Selan C, Chia JSJ, Sturgeon SA, Wright DK, Zamani A, Pereira M, Nandurkar HH, Sashindranath M (2020) Characterization of a novel model of global forebrain ischaemia-reperfusion injury in mice and comparison with focal ischaemic and haemorrhagic stroke. *Sci Rep* 10:18170.
 44. Covington HE 3rd, Lobo MK, Maze I, Vialou V, Hyman JM, Zaman S, LaPlant Q, Mouzon E, Ghose S, Tamminga CA, Neve RL, Deisseroth K, Nestler EJ (2010) Antidepressant effect of optogenetic stimulation of the medial prefrontal cortex. *J Neurosci* 30:16082-16090.
 45. Capuzzo G, Floresco SB (2020) Prelimbic and infralimbic prefrontal regulation of active and inhibitory avoidance and reward-seeking. *J Neurosci* 40:4773-4787.
 46. Corcoran KA, Quirk GJ (2007) Activity in prelimbic cortex is necessary for the expression of learned, but not innate, fears. *J Neurosci* 27:840-844.
 47. Soler-Cedeño O, Cruz E, Criado-Marrero M, Porter JT (2016) Contextual fear conditioning depresses infralimbic excitability. *Neurobiol Learn Mem* 130:77-82.
 48. Suzuki S, Saitoh A, Ohashi M, Yamada M, Oka J, Yamada M (2016) The infralimbic and prelimbic medial prefrontal cortices have differential functions in the expression of anxiety-like behaviors in mice. *Behav Brain Res* 304:120-124.
 49. Fuchikami M, Thomas A, Liu R, Wohleb ES, Land BB, DiLeone RJ, Aghajanian GK, Duman RS (2015) Optogenetic stimulation of infralimbic PFC reproduces ketamine's rapid and sustained antidepressant actions. *Proc Natl Acad Sci U S A* 112:8106-8111.
 50. Wang M, Perova Z, Arenkiel BR, Li B (2014) Synaptic modifications in the medial prefrontal cortex in susceptibility and resilience to stress. *J Neurosci* 34:7485-7492.
 51. Poorthuis RB, Bloem B, Schak B, Wester J, de Kock CP, Mansvelder HD (2013) Layer-specific modulation of the prefrontal cortex by nicotinic acetylcholine receptors. *Cereb Cortex* 23:148-161.
 52. Soares LM, Schiavon AP, Milani H, de Oliveira RM (2013) Cognitive impairment and persistent anxiety-related responses following bilateral common carotid artery occlusion in mice. *Behav Brain Res* 249:28-37.
 53. Kim JH, Ko PW, Lee HW, Jeong JY, Lee MG, Kim JH, Lee WH, Yu R, Oh WJ, Suk K (2017) Astrocyte-derived lipocalin-2 mediates hippocampal damage and cognitive deficits in experimental models of vascular dementia. *Glia* 65:1471-1490.
 54. Lee TK, Kim H, Song M, Lee JC, Park JH, Ahn JH, Yang GE, Kim H, Ohk TG, Shin MC, Cho JH, Won MH (2019) Time-course pattern of neuronal loss and gliosis in gerbil hippocampi following mild, severe, or lethal transient global cerebral ischemia. *Neural Regen Res* 14:1394-1403.
 55. Kim DH, Choi BR, Jeon WK, Han JS (2016) Impairment of intradimensional shift in an attentional set-shifting task in rats with chronic bilateral common carotid artery occlusion. *Behav Brain Res* 296:169-176.
 56. Eichenbaum H (2017) Prefrontal-hippocampal interactions in episodic memory. *Nat Rev Neurosci* 18:547-558.
 57. Jefferson T, Kelly CJ, Martina M (2021) Differential rearrangement of excitatory inputs to the medial prefrontal cortex in chronic pain models. *Front Neural Circuits* 15:791043.
 58. Anastasiades PG, Carter AG (2021) Circuit organization of the rodent medial prefrontal cortex. *Trends Neurosci* 44:550-563.
 59. Michalettos G, Ruscher K (2022) Crosstalk between GABAergic neurotransmission and inflammatory cascades in the post-ischemic brain: relevance for stroke recovery. *Front Cell Neurosci* 16:807911.

60. Clarkson AN, Huang BS, Macisaac SE, Mody I, Carmichael ST (2010) Reducing excessive GABA-mediated tonic inhibition promotes functional recovery after stroke. *Nature* 468:305-309.
61. Soumier A, Sibille E (2014) Opposing effects of acute versus chronic blockade of frontal cortex somatostatin-positive inhibitory neurons on behavioral emotionality in mice. *Neuropsychopharmacology* 39:2252-2262.
62. Perova Z, Delevich K, Li B (2015) Depression of excitatory synapses onto parvalbumin interneurons in the medial prefrontal cortex in susceptibility to stress. *J Neurosci* 35:3201-3206.
63. Fan Z, Chang J, Liang Y, Zhu H, Zhang C, Zheng D, Wang J, Xu Y, Li QJ, Hu H (2023) Neural mechanism underlying depressive-like state associated with social status loss. *Cell* 186:560-576.e17.
64. Ruan L, Wang Y, Chen SC, Zhao T, Huang Q, Hu ZL, Xia NZ, Liu JJ, Chen WJ, Zhang Y, Cheng JL, Gao HC, Yang YJ, Sun HZ (2017) Metabolite changes in the ipsilateral and contralateral cerebral hemispheres in rats with middle cerebral artery occlusion. *Neural Regen Res* 12:931-937.